The elastic uniaxial properties of a centre symmetric honeycomb with curved cell walls: effect of density and curvature

E. Harkati[1], N. Daoudi[1], C. Abaidia[1], A. Bezazi[2], F. Scarpa[3]

[1.] Laboratoire des Mines Université Tébessa, Route de Constantine 12000-Tébessa, Algérie
[2.] Laboratoire de Mécanique appliquée des nouveaux matériaux (LMANM), Bp 401 Université de 8 Mai 1945 Guelma, Algeria.
[3.] Advanced Composites Centre for Innovation and Science (ACCIS), University of Bristol, BS8 1TR Bristol, UK

Abstract

We propose in this paper analytical and numerical models that describes the in-plane uniaxial elastic properties (Young's moduli and Poisson's ratios) of a honeycomb structure with curved walls. We perform a parametric analysis of the mechanical performance of this honeycomb also by taking into account the different types of deformations acting inside the cell walls. The curved wall honeycomb possesses higher magnitudes of the Poisson's ratio ν_{12} in the auxetic configuration compared to classical centre symmetric configuration with straight cell wall. The presence of the curvature also allows creating configurations with positive Poisson's ratio even for negative internal cell angles, and makes this honeycomb design attractive for mechanical tailoring.

Keywords: Auxetic; Honeycomb; Homogenization; negative Poisson's ratio; Finite element; refined model.

Corresponding author: Prof. Abderrezak BEZAZI, Laboratoire de Mécanique appliquée des nouveaux matériaux (LMANM), Bp. 401 Université de 8 Mai 1945 Guelma, Algeria.
E-mail: ar_bezazi@yahoo.com

Phone : +213 667 72 88 99

I. Introduction

Cellular materials have witnessed a remarkable diffusion during the past fifty years in terms of development and applications. These low-density materials are widely used mainly because of their high rigidity/weight ratio. During the last twenty years in particular, the production and use of cellular materials have increased significantly in various domains (from transport to packaging and aerospace) [1]. A number of studies have been published in recent years on cellular structures, especially on 2D honeycombs [2][3][4] with the capacity of showing an in-plane negative Poisson's ratio (i.e., auxetic behaviour). Poisson's ratio is defined as the ratio between the lateral and axial deformations under uniaxial tensile loading, with the sign minus. In most cases, the Poisson's ratio ν is positive, i.e. the material undergoes a contraction in the direction perpendicular to the direction of the effort applied. On the contrary, a material with a negative Poisson's ratio laterally expands when elongated, leading to an increase of its volume. Gibson and Ashby [2] identified the presence of an in-plane negative Poisson's ratio in centre

symmetric configurations. While the basic bending deformation mechanism of the wall is conducive to a negative Poisson's ratio when the internal angle of the cell is negative [2], other authors have identified the importance of stretching and hinging deformations in the performance of the in-plane mechanical properties of these honeycombs [5]. Several researchers have formulated mathematical models based on these mechanisms [2]-[6], all assuming that engineering beams constituted the cell walls. Some researchers [5] have also showed that models based only on bending deformations overestimated the values of elastic moduli, compared to those provided by molecular modelling. The analysis presented in this work focuses on a centre symmetric honeycomb configuration represented in Fig. 1, which possesses a curved wall. The presence of the curved geometry induces in the structure a series of deformations associated to bending, stretching and hoop stresses, and therefore gives the opportunity of increasing the availability of tailored mechanical properties. The presence of the curvature inside the wall may take into account some real manufacturing constraints related to the use of over-expanded [7] and composite Kirigami techniques [8][9] in which the intersection between ribs is not represented by a sharp angle. Moreover, special geometries of the ribs at the intersection between different cell walls do tend to provide tailored deformation mechanisms to the global honeycomb cell [10], and are considered responsible for unusual mechano-thermal behaviour like the blocked shape memory effect observed in open cell PU foams subjected to multiple shape memory training [11].

The mechanical properties of curved (sinusoidal) ligaments of auxetic structures that have been subjected to large deformations has been studied by Strek *et al* [12][Str2016]. For each of the four structures considered, the impact of the deformation size and geometrical parameters on the effective mechanical properties of the structures shape have been investigated. It has been shown that some of them are auxetic when compressed and non-auxetic when stretched. Hence, a smart control of the mechanical properties of the sinusoidal ligament structure can be performed through its geometry and arrangement of ligaments. The analytical expressions derived by Grima *et al* [13] [GRI2013] suggests that hexagonal truss systems made from ribs having different stretching stiffness constants exhibit a negative compressibility in the vertical direction for particular re-entrant geometries of this smart hexagonal truss system when the vertical ribs are much stiffer than the inclined ones. Poziniak *et al.* [14][Poz2013] carried out a numerical simulation on two cellular two-dimensional auxetic foams with modified joints of simple cells referred to as Y- and Δ-models. For the first model, the ribs forming the cells are connected at points corresponding to sites of a disordered honeycomb lattice, whereas for the second, the connections of the ribs are not point-like but spatial. The simulations show that by applying harder joints, lower Poisson's ratios can be reached. It also shows that the Δ-model gives lower Poisson's ratios than the Y-model. In order to evaluate its dynamic response properties, a numerical simulation of a sandwich panel constituted by two face sheets and auxetic hexagonal re-entrant structure core has also been carried out by Strek *et al* [15] [Str 2015]. The results showed that the effective Young's modulus of such sandwich panels becomes very large if the Poisson's ratio of the filler material tends to -1. In order to minimize the effective Poisson's ratio of the sandwich panel's core, another numerical analysis using a finite-element approach combined with an optimization algorithm MMA (method of moving asymptotes) was performed by Strek *et al* [16] [Str2016] who found that the composite structure exhibits a negative Poisson's ratio (NPR) while a positive one characterizes all its constituents. Lakes [17] [Lakes 1987] has been the first to produce isotropic auxetic foams from conventional low-density open-cell polymer foams by causing the ribs of each cell to permanently protrude inward. He also stated that the Poisson's ratio in materials is essentially governed by the presence of microstructure properties represented by rotational degrees of freedom, anisotropic structure as well as non-affine deformation kinematics that are seen to be essential for the

production of negative Poisson's ratios for isotropic materials containing central force linkages of positive stiffness [18] [LAK 1991].

Sigmund [19] Sig 1994 has formulated the so-called inverse problem by as a two-dimensional topology optimization problem where the cost is minimized and the constraints defined by the prescribed constitutive parameters through finding the interior topology of a base cell. The obtained numerical results show that arbitrary materials, including materials with Poisson's ratio equals - 1.0 and other extreme materials, can be obtained by modelling the base cell as a truss structure. Provided that the ligament length to thickness ratio remains sufficiently large and the overall length to width ratio of the disordered system does not differ considerably from that of its ordered counterpart, Mizi *et al* [20] noted that the transitional disorder in the hexachiral honeycombs has no significant effect on the Poisson's ratio. However, the Young's modulus of the system increases along with the extent of disorder. Moreover and unlike other auxetic geometries, the hexachiral honeycomb system is found to be extremely tolerant to translational disorder and possesses the outstanding capability of retaining more or less its original Poisson's ratio despite degrees of disorder of up to 90%. The numerical simulations accomplished by means of finite-element analysis of a segment of a composite sandwich panel built of two constituent materials of different thermomechanical properties has been performed by Jopek and Strek [21] JOp 2015, and showed that it is possible to obtain a material that exhibits auxetic behaviour although all its constituents does not. Furthermore, the smallest values of the effective Poisson's ratio are obtained for the most elongated elliptical shape where the semi-minor axis $R_1 = 0.11$. However and as the shape of the fibers becomes more elliptical, the geometry of the composite core tends to be more similar to the well-known auxetic geometry of rotating squares. The work of Grima *et al* [22] [GRi2016] explored the mechanical behavior of slit-perforated systems where the highly ordered pattern of slits in traditional auxetic perforated systems are replaced by an arrangement where each slit is oriented in a quasi-random manner. The investigation was performed using a Finite Element approach and showed that a regular conventional sheet of rubber-like material can be converted into a more value-added auxetic metamaterial with high negative Poisson's ratios through the introduction of non-symmetric quasi-random cuts. Pozniak *et al* [23] [Poz2016] performed finite element studies focusing on effective mechanical properties of systems with elliptic inclusions in order to investigate the effective Poisson's ratio and Young's modulus corresponding to stresses acting in the x-axis direction. The authors concluded that for very soft inclusions, the dominating mechanism is that of rotating rigid units that leads to almost perfect auxeticity (Poisson's ratios close to -1). However, for the opposite limit (for rigid inclusions), the auxeticity has also been observed. Wojciechowski [24] [Woj1987] applied a constant thermodynamic tension Monte Carlo method in order to study the elastic properties of a two-dimensional system of hard cyclic hexamers at different pressure values. He found that the Poisson modulus could be negative in the tilted phase. In another study, the same author [25] [Woj1989] showed that a two-dimensional lattice model of hexagonal molecules on a triangular lattice interacting via a nearest-neighbour n-inverse-power site-site potential displays a negative Poisson's ratio at high densities when the anisotropy of the molecules is large. Mechanisms leading to a planar negative Poisson's ratio consisting of a simple structure formed by squares, which can be regarded as a crystal structure, where each square can only rotate was proposed by Ishibashi and Iwata [26] [Ish2000].

In order to derive the Poisson's ratio, the elastic compliances of a two-dimensional model systems of hard discs with parallel layers of hard cyclic hexamers were determined by Bilski and Wojciechowski [27] [Bil2016] using a Monte Carlo simulation in the isobaric–isothermal ensemble with variable shape of the periodic box. At the same concentrations, the systems with

H-layers showed significantly lower values of Poisson's ratio than those with V-layers thus strongly depending on the layer orientation. The obtained results indicate a new way for modifying crystal Poisson's ratios.

The aim of this paper is to propose a new refined analytical model capable of evaluating the effect of relative density and curvature of cell walls on the mechanical properties of periodic honeycomb cells with round corners. In order to find out the optimal topologies for different multifunctional applications, the anisotropic behaviour of honeycomb materials at round corners must be described using all three deformations (flexural, shear and stretching mechanisms). In addition, a numerical model using Abacus software is developed to validate the analytical established approach. It is worth noticing that this investigation is a continuation of the previous one performed by Bezazi *et al.* [10].

Nomenclature

t : *thickness of the cell wall*
l : *lengths of the cell walls*
a : *length of the base wall*
b : *height of the cell*
θ : *internal angle of the cell*
P : *concentrated load along the direction 1*
W : *concentrated load along the direction 2*
u^M : *displacement due to bending*
u^N : *displacement due to axial force*
u^T : *displacement due to shear*
U : *strain Energy*
E_s : *Young's modulus of the constituent material*
E_1,E_2 : *Young's modulus in the direction 1 and 2*
G_s : *Shear modulus*
v : *Poisson's ratio of the constituent material*
v_{12}, v_{21} : *theoretical in-plane Poisson's ratios*
A^* : *reduced shear section*
ε_1, ε_2 : *in-plane strains*
$\alpha = \frac{r}{l}$: *curved cell walls aspect ratio*
$\beta = \frac{a}{l}$: *base wall aspect ratio*
$\gamma = \frac{t}{l}$: *honeycomb relative density*

II. Analytical models

The actual developed analytical model is linked to the prediction of the mechanical properties in honeycomb cores illustrated in [2][5][10][28][29]. The novelty relies on taking into account the strain energy associated with the shear and the axial (stretching) force acting in the walls. Fig. 1 presents a honeycomb design in which the sharp edge corners are replaced by round shapes. In the following analytical development, the radius r is considered a variable together with the length a.

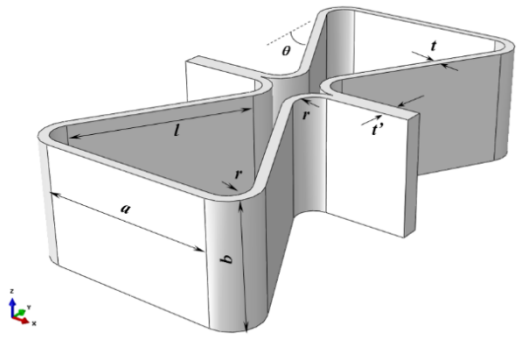

Fig. 1. New design of the re-entrant cell

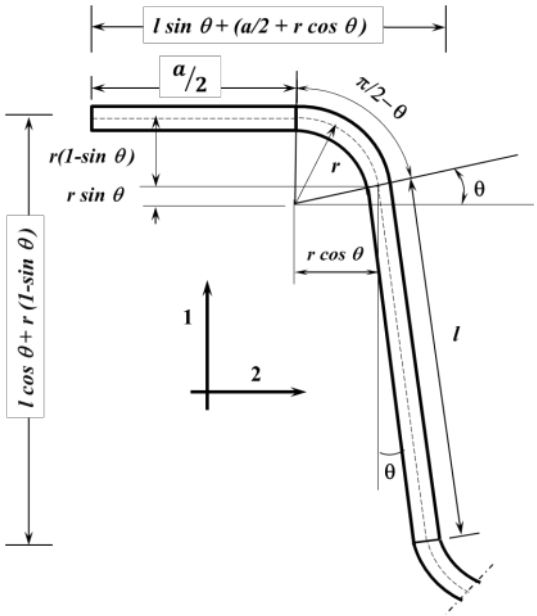

Fig .2 Detail of the geometry at the corner of the new curved honeycomb.

In the design of cellular materials, the density ratio ρ/ρ_s is an important parameter [2] and it can be calculated as:

$$\frac{\rho}{\rho_s}=\frac{1}{2}t\frac{\left(a+2l-2r\theta+\pi r\right)}{\left(a+2r\cos\theta+l\sin\theta\right)\left(2r+l\cos\theta-2r\sin\theta\right)} \tag{1}$$

Using non-dimensional parameters to define the geometry of the unit cell similarly to the ones used in [2][29], Eq. (1) can be recast as:

$$\frac{\rho}{\rho_s}=\frac{1}{2}\gamma\frac{\left(2\beta+2+\alpha(\pi-2\theta)\right)}{\left(\beta+2\alpha\cos\theta+\sin\theta\right)\left(2\alpha+\cos\theta-2\alpha\sin\theta\right)} \tag{2}$$

With $\alpha=\frac{r}{l};\beta=\frac{a}{l};\gamma=\frac{t}{l}$

It is worth noticing that by reducing the radius *r* to zero, one would obtain the density ratio for classical centre symmetric configurations [1].

II.1 Refined analytical model

The theorem of Castigliano's is used to develop the present analytical model by considering the effect of bending, shear and stretching deformations on the honeycomb struts. This theorem states that the potential strain energy stored in the beam is given by:

$$U=\frac{1}{2}\iiint\left(\sigma_{xx}\varepsilon_{xx}+\sigma_{yy}\varepsilon_{yy}+\sigma_{zz}\varepsilon_{zz}+\tau_{xy}\gamma_{xy}+\tau_{xz}\gamma_{xz}+\tau_{yz}\gamma_{yz}\right)dV \tag{3}$$

The same methodology used by Bezazi *et al.* [10] is adapted to calculate the homogenized in-plane mechanical properties of the actual honeycomb with round corners (Fig. 2).

By using the unit load method [10], the unit cell deformation along the 1-direction due to bending can be calculated as (after simplifications and using the non-dimensional parameters):

$$u_1^M = \frac{Pl^3}{12E_s I}\begin{pmatrix} 6\left(\pi-2\theta-8\cos\theta+6\cos\theta\sin\theta+(2\pi-4\theta)\cos^2\theta\right)\alpha^3 \\ +12\left(2-2\sin\theta-2\cos^2\theta+(\pi-2\theta)\cos\theta\sin\theta\right)\alpha^2 \\ +3\left(\pi-2\theta-(\pi-2\theta)\cos^2\theta\right)\alpha+\sin^2\theta \end{pmatrix} \quad (4)$$

The normal (axial) forces lead to an extension in the oblique wall (straight and curved parts) and the overall extension for the unit cell in the direction 1 can be determined as:

$$u_1^N = \frac{Pl}{2E_s A}\left(1-2\alpha\theta+\cos 2\theta-\alpha\sin 2\theta+\pi\alpha\right) \quad (5)$$

The transverse shear force contribution to the cross-section deformation of the beam of the unit cell is given by:

$$u_1^T = \frac{Pl}{2G_s A^*}(1-2\alpha\theta-cos2\theta+\alpha sin2\theta+\pi\alpha) \quad (6)$$

This equation predicts the shear deformation for a rectangular cross-section with a shear correction factor of 1. The corresponding correction factor for a rectangular cross-section should be 1.2 [29], but it is assumed that the shape variation in the curved portions of the unit cell reduces it back to 1. The shear modulus for the wall materials is equal to:

$G_s = \frac{E_s}{2(1+\nu)}$, where ν is the Poisson's ratio of the core material, together with $A = bt$; $A^* = \frac{5}{6}bt$; $I = \frac{bt^3}{12}$. The total unit cell deformation along direction 1 is given by the sum of the extension, shear and bending components of the deformation:

$$u_1 = u_1^M + u_1^N + u_1^T \quad (7)$$

The elastic modulus in the direction 1 is calculated following the classical Gibson's and Ashby's approach [2] with the stress σ_1 representing the external load on the unit cell:

$$\sigma_1 = \frac{P}{b(a+l\sin\theta+2r\cos\theta)} \quad (8)($$

In (8), *b* represents the height of the honeycomb along the out-of-plane direction. For the unit cell, the strain ε_1 is calculated as:

$$\varepsilon_1 = \frac{u_1}{l\cos\theta+2r(1-\sin\theta)} \quad (9)$$

The homogenized Young's modulus E_1 will therefore be calculated as the ratio between the tensile stress σ_1 and the strain ε_1:

$$\frac{E_1}{E_s} = \frac{\cos\theta+2\alpha(1-\sin\theta)}{\beta+\sin\theta+2\alpha\cos\theta}\frac{1}{\bar{u}_1} \quad (10)$$

where:

$$\bar{u}_1 = \frac{1}{\gamma^3}\left[\begin{pmatrix} 6\left(\pi-2\theta-8\cos\theta+6\cos\theta\sin\theta+(2\pi-4\theta)\cos^2\theta\right)\alpha^3 \\ +12\left(2-2\sin\theta-2\cos^2\theta+(\pi-2\theta)\cos\theta\sin\theta\right)\alpha^2 \\ +3\left(\pi-2\theta-(\pi-2\theta)\cos^2\theta\right)\alpha+\sin^2\theta \end{pmatrix} + \begin{pmatrix} \frac{1}{2}\gamma^2\left(1-2\alpha\theta+\cos 2\theta-\alpha\sin 2\theta+\pi\alpha\right) \\ +\frac{6(1+\nu)}{5}\gamma^2\left(1-2\alpha\theta-\cos 2\theta+\alpha\sin 2\theta+\pi\alpha\right) \end{pmatrix}\right] \quad (11)$$

For a regular cell ($\alpha=0$), the expression related to the centre-symmetric honeycomb with straight beams and combined bending/stretching/shear deformation is expressed as [2]:

$$\frac{E_1}{E_s} = \gamma^3 \frac{\cos\theta}{(\beta+\sin\theta)\sin^2\theta}\left(\frac{1}{1+\gamma^2(\cot^2\theta+\frac{12}{5}(\nu+1))}\right) \tag{12}$$

For the elastic modulus along the direction 2, the assumptions and methodology adopted in paragraph II are used. The deformation used to bending the cell wall under a transverse load W is expressed as:

$$u_2^{\ M} = \frac{Wl^3}{12E_sI}\begin{bmatrix} 6(2\pi-4\theta-3\sin 2\theta-\pi\cos 2\theta+2\theta\cos 2\theta)\alpha^3 \\ +6(2\cos 2\theta-\pi\sin 2\theta+2\theta\sin 2\theta+2)\alpha^2 \\ +\frac{3}{2}(\cos 2\theta+1)(\pi-2\theta)\alpha \\ +\cos^2\theta \end{bmatrix} \tag{13}$$

The overall stretching deformation for the unit cell along the direction 2 is calculated as:

$$u_2^N = \frac{Wl}{2E_sA}(1-2\alpha\theta-cos2\theta+\alpha sin2\theta+\pi\alpha) \tag{14}$$

The shear deformation cross-section contribution is:

$$u_2^T = \frac{W}{2G_sA^*}\left(2l\cos^2\theta - 2r\theta - r\sin 2\theta + \pi r\right) \tag{15}$$

The total unit cell deformation along direction 2 is given by the sum of the extension, shear and bending components of the cell wall deformation:

$$u_2 = u_2^M + u_2^N + u_2^T \tag{16}$$

The stress along direction 2 is expressed as:

$$\sigma_2 = \frac{W}{b(l\cos\theta+2r(1-\sin\theta))} \tag{17}$$

The strain ε_2 has the following formulation:

$$\varepsilon_2 = \frac{u_2}{a+l\sin\theta+2r\cos\theta} \tag{18}$$

The elastic modulus along direction 2 is expressed as the ratio between the applied stress and the effective strain of the unit cell:

$$\frac{E_2}{E_s} = \frac{\beta+\sin\theta+2\alpha\cos\theta}{\cos\theta+2\alpha(1-\sin\theta)}\frac{1}{\bar{u}_2} \tag{19}$$

where:

$$\bar{u}_2 = \frac{1}{\gamma^3}\left[\begin{bmatrix} (12\pi-24\theta-18\sin 2\theta-6\pi\cos 2\theta+12\theta\cos 2\theta)\alpha^3 \\ +(12+12\cos 2\theta-6\pi\sin 2\theta+12\theta\sin 2\theta)\alpha^2 \\ +(\frac{3}{2}\pi-3\theta+\frac{3}{2}\pi\cos 2\theta-3\theta\cos 2\theta)\alpha \\ +\cos^2\theta \end{bmatrix} + \begin{Bmatrix} \frac{1}{2}\gamma^2(1-2\alpha\theta-\cos 2\theta+\alpha\sin 2\theta+\pi\alpha+4\beta) \\ +\frac{6(1+\nu)}{5}\gamma^2(2\cos^2\theta-2\alpha\theta-\alpha\sin 2\theta+\pi\alpha) \end{Bmatrix}\right] \tag{20}$$

Also in this case, it may be noticed that when $\alpha = 0$ one obtains the result related to a unit cell with straight beams:

$$\frac{E_2}{E_s} = \gamma^3 \frac{\beta+\sin\theta}{\cos^3\theta}\left(\frac{1}{1+\gamma^2\left(\frac{2\beta}{\cos^2\theta}+\tan^2\theta+\frac{12}{5}(v+1)\right)}\right) \tag{21}$$

II.3 Poisson's ratio

The Poisson's ratio υ_{12} can be computed by following the classical formulation:

$$\upsilon_{12} = -\frac{\varepsilon_2}{\varepsilon_1} \tag{22}($$

Substituting equations (9) and (18) into (22) and simplifying, one obtains:

$$\nu_{12} = -\frac{\cos\theta+2\alpha(1-\sin\theta)}{\beta+\sin\theta+2\alpha\cos\theta}\frac{\overline{u}_{2-1}}{\overline{u}_{1-1}} \tag{23}$$

When the load has been applied to the same direction, the total displacement along the direction 1 is represented by:

$$\overline{u}_{1-1} = \frac{1}{\gamma^3}\left[\begin{bmatrix}(24\sin\theta-6+18\cos2\theta-6\pi\sin2\theta+12\theta\sin2\theta)\alpha^3\\+(12\sin2\theta-12\cos\theta+6\pi\cos2\theta-12\theta\cos2\theta)\alpha^2\\+\left(\frac{3}{2}\pi\sin2\theta-3\theta\sin2\theta\right)\alpha\\+\frac{1}{2}\sin2\theta\end{bmatrix}+\begin{pmatrix}-\frac{1}{2}\gamma^2(\alpha+\alpha\cos2\theta+\sin2\theta)\\+\frac{6(1+\nu)}{5}\gamma^2(\alpha+\alpha\cos2\theta+\sin2\theta)\end{pmatrix}\right] \tag{24}$$

The analogous displacement along the direction 2 becomes:

$$\overline{u}_{2-1} = \frac{1}{\gamma^3}\left[\begin{bmatrix}6(\pi-2\theta-8\cos\theta+6\cos\theta\sin\theta+2\pi\cos^2\theta-4\theta\cos^2\theta)\alpha^3\\12(-2\sin\theta-2\cos^2\theta+\pi\cos\theta\sin\theta-2\theta\cos\theta\sin\theta+2)\alpha^2\\(3\pi-6\theta-3\pi\cos^2\theta+6\theta\cos^2\theta)\alpha+\sin^2\theta\end{bmatrix}+\begin{pmatrix}\frac{1}{2}\gamma^2(1-2\alpha\theta+\cos2\theta-\alpha\sin2\theta+\pi\alpha)\\+\frac{6(1+\nu)}{5}\gamma^2(1-2\alpha\theta-\cos2\theta+\alpha\sin2\theta+\pi\alpha)\end{pmatrix}\right] \tag{25}$$

With $\alpha = 0$, one can reach the results of a centre symmetric cell with straight ligaments [2]:

$$\nu_{12} = -\frac{\cos^2\theta}{(\beta+\sin\theta)\sin\theta}\frac{\left[1-\gamma^2+\frac{12}{5}\gamma^2(v+1)\right]}{\left[1+\gamma^2\cot^2\theta+\frac{12}{5}\gamma^2(v+1)\right]} \tag{26}$$

By making use of the cross-product of Young's moduli and Poisson's ratios for special orthotropic materials one can calculate the Poisson's ratio v_{21} as:

$$v_{21} = \frac{E_1}{E_2}v_{12} \tag{27}$$

III. Finite element model

A Finite Element model has been developed to simulate the elastic constants of the honeycomb by using an asymptotic homogenization approach [31][32]. The model was developed with the Abaqus 6.10 [33] commercial code. An assembly of 133 cells constitutes the finite element model representing the elementary volume (RVE) of the honeycomb structure after convergence shown in Fig. 3. For the FE models, an elastic shell element with reduced integration 90120 elements (S4R) was used. The discretization corresponded to 20 elements per unit length *a*. For the calculation of the various elastic modules, a displacement is imposed on one side of the RVE. For the calculation of the various modules, a displacement is imposed

on one side of the RVE along the loading direction, the opposite side being fixed. Symmetries are taken into account in the boundary conditions to compute the different elastic constants.

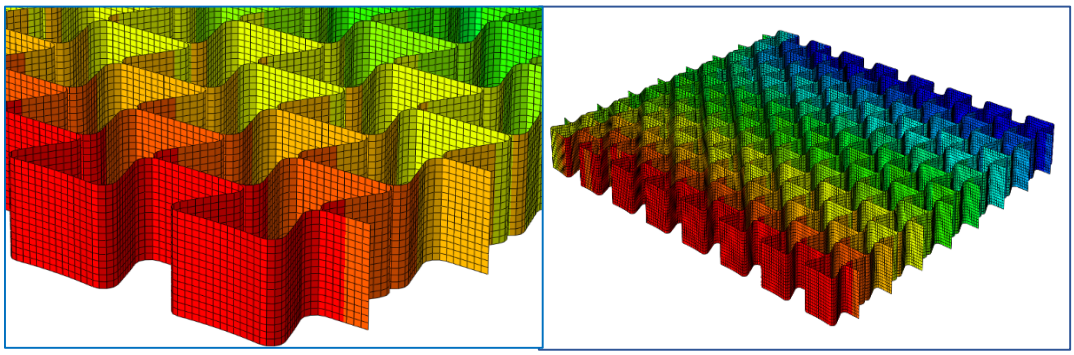

Fig.3 Representative volume element(RVE)

IV. Results and discussions

IV.1. Analysis of the analytical results

The mechanical performance of the new curved honeycomb configurations is discussed by introducing the effect of the bending moment (M), shear (T) and the normal force (N) in the deformation mechanisms of the honeycomb cell wall. The contribution of the wall cross-section defined by the dimensionless ratio $\gamma = t/l$ is considered.

Fig. 4 shows the variation of the effective modulus E_1 with the different deformation mechanisms in the wall MNT for two values of γ corresponding to a thin cell wall ($\gamma = 0.1$) and a thicker one ($\gamma = 0.2$). For the case of the thin wall, one can observe a slight difference between the contribution given by the different deformation mechanisms in the vicinity of $\theta = 0°$ which decreases significantly for angles exceeding ± 10 °. A stronger contribution from the bending mechanism is observed for the thick wall. This is particularly evident when observing Fig.4 in which the bending provides a 7-times higher contribution than other deformation mechanisms at low cell θ angles. Any other deformation mechanism contribution tends to lower the response provided by the cell walls under pure bending loading (Fig. 4). The consideration of the influence of shear and axial strains (N, T) are however usually overlooked [2][32] because of their low contributions in the evaluation of the cell elastic constants especially for larger internal cell angles. The results show that the effect of N and T becomes significant if the thickness parameter $\gamma = t/l$ exceeds 0.2 with the other dimensionless parameters being kept constant ($\alpha = 0.1$, $\beta = 1$).

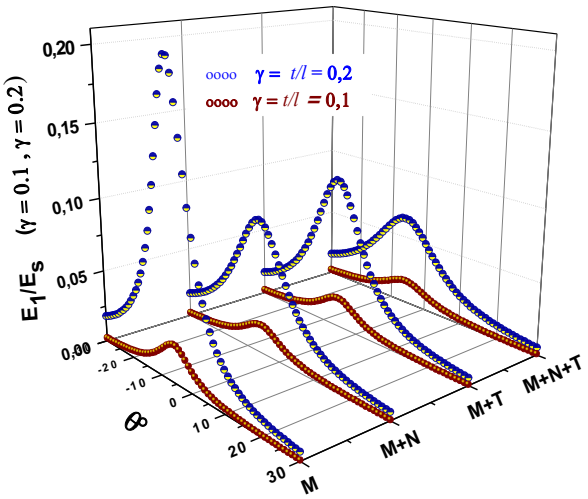

Fig 4. The effect of the different combinations of deformation on the elastic moduli along direction 1;

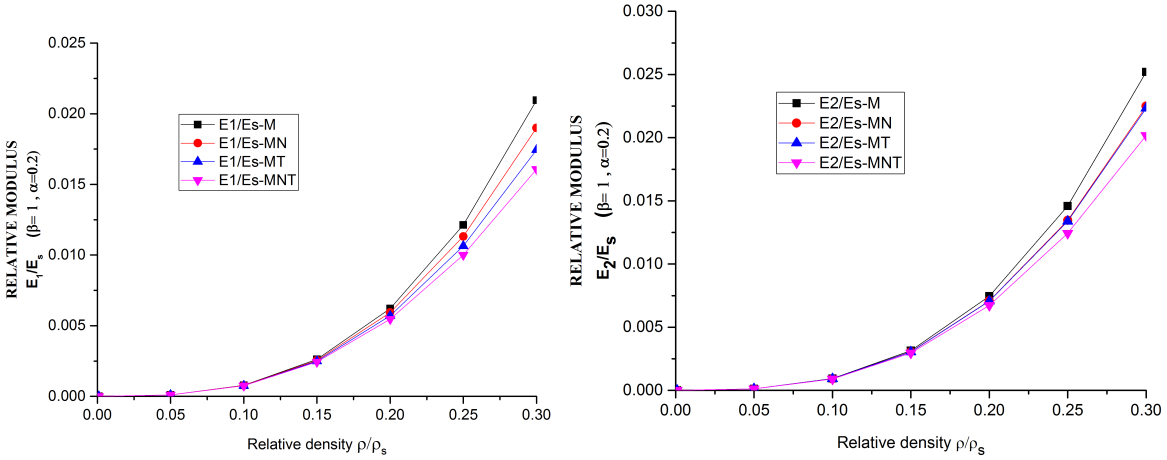

α =0.2, β = 1, θ = 30

Fig .5: Non-dimensional Young's moduli versus the relative density for different combinations of deformation mechanisms

(a) E_1/Es depending on ρ/ρ_s

(b) E_2/Esdepending on ρ/ρ_s

Fig. 5 shows the variation of the non-dimensional moduli E_1/E_s and E_2/E_s versus the relative density for four different combinations of the deformation mechanisms acting in the cell wall. The two non-dimensional moduli increase monotonically with a maximum relative density of 0.3. At lower relative densities, the four combinations of deformation mechanisms do not provide a tangible difference between the moduli. On the opposite and at higher relative densities, it is possible to observe that the separate deformation mechanism do affect the stiffness in a sensible way. For a relative density ρ/ρ_s of 0.25 and if the bending deformation mechanism is considered as the dominant one, the dimensionless modulus E_1/E_S is 1.3 times higher than when all the deformation mechanisms are taken into account. As shown in Figure 5b, the same observations can be made for the ratio E_2/E_S. It is clear that the analytical model that takes into account the bending deformation mechanism solely overestimates the stiffness in both directions for relative densities higher than 0.2. For lower densities, the effect of the different mechanisms is almost negligible.

For a positive internal cell angle $\theta = 30°$, the increase of the relative density of the cell reduces the Poisson's ratio to 0.8 for a relative density of 0.3 with $\alpha = 0.1$, $\beta = 1$ (Figure 6). Note that when using an analytical model that considers the bending deformation mechanism only (*M*), the variation of the relative density does not affect the Poisson's ratio ν_{12} that becomes constant at 0.83 (Figure 6-a). It is also worth noticing that in the refined model with all deformation mechanisms included (*MNT*) and for a re-entrant cell ($\theta = -30°$), the auxetic behaviour is remarkable on the Poisson's ratios values, starting from $v_{12} = -3.4$ at low relative densities and passing to $v_{12} = -3.2$ for a relative density of 0.3 (Figure 6-b). For the other combinations, the variation is less important.

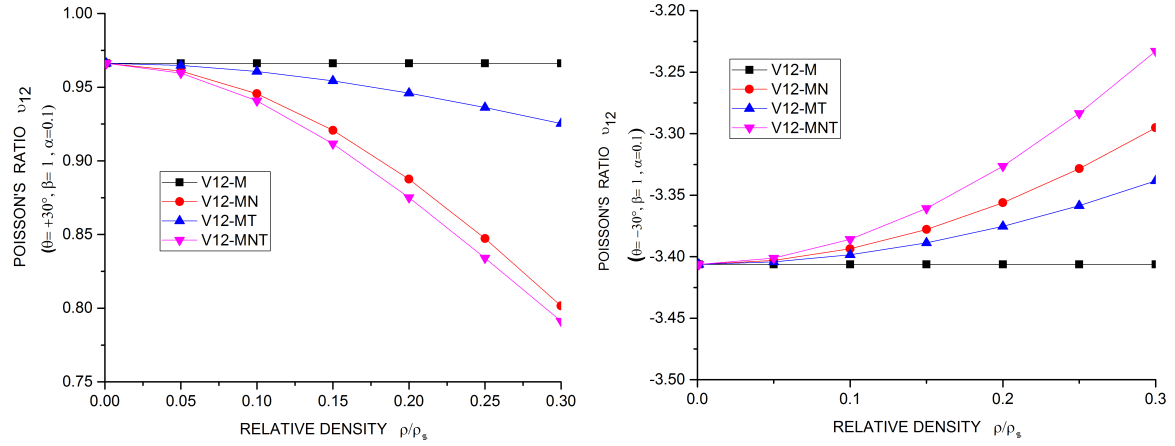

(a) (b)

Fig.6: The effect of the contribution of the MNT deformation mechanisms on the Poisson ν_{12} (α =0.1, β = 1) with:

(a) : θ = 30 , (b) : θ = -30

The evolution of the dimensionless elasticity modulus E_1/E_s as a function of the relative density for different values of α (0.1, 0.2, 0.3 and 0.4) is shown in Figure 7a. The non-dimensional modulus E_1/E_s increases with higher curvature radius α. For example, an increase of 40% is observed on E_1/E_s if the curvature ratio α moves from 0.1 to 0.4. Figure7-b also shows that the elasticity modulus E_2/E_s is relatively dependent on the radius of curvature ratio α, although at a lesser extent.

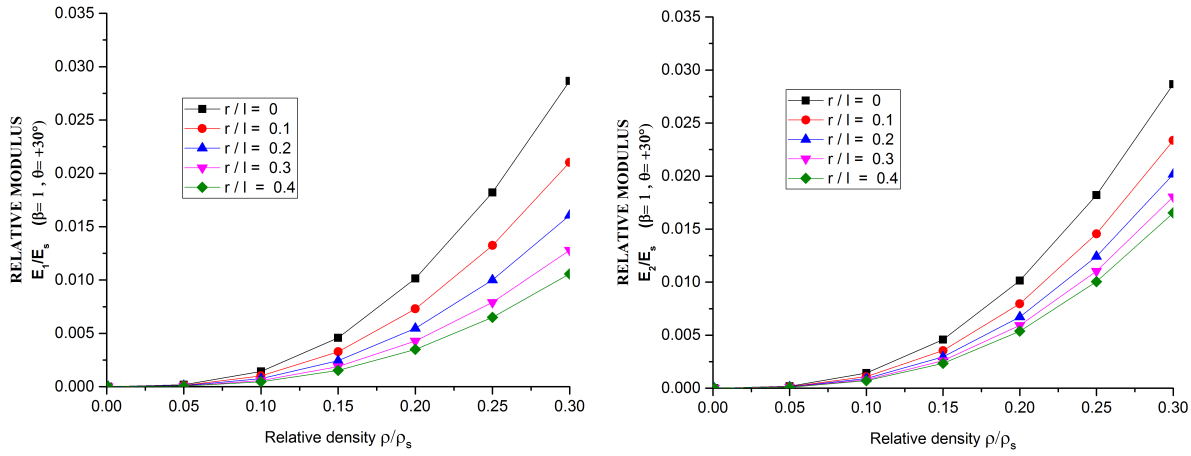

(a) (b)

Fig 7: Non-dimensional Young's moduli in terms of the relative density: ($\theta = 30°$ and $\beta = 1$)

(a) E_1/Es depending on ρ/ρ_s and α

(b) E_2/Es depending on ρ/ρ_s and α

The evolution of the Poisson's ratio in terms of the relative density of the honeycomb cell for different curvature ratios is shown in Figure 8. For the positive cell internal angle $\theta = 30°$, we observe (as expected) a positive Poisson's ratio. Conversely, an auxetic behaviour is observed for a negative angle $\theta = -30°$. In this case, Poisson's ratio ν_{12} exceeds -4 for low relative densities (Figure 8.b). This figure takes into consideration all the deformation mechanisms (MNT) acting in the ribs.

From observing Figure 8.a, it can be noticed that for a positive internal cell angle $\theta = +30°$ the increase of the relative density of the cell reduces the Poisson's ratio to a value of $\nu_{12} = 0.8$ for a relative density of 0.4 and a relative radius of curvature $r/l = 0.2$. On the opposite and for a reentrant cell ($\theta = -30°$), the auxetic behavior decreases for high relative densities. In this case, the Poisson's ratio decreases to $\nu_{12} = -3.9$ for a curvature ratio $r/l = 0.2$ and a low relative density from 0.05. A higher relative density (0.3) tends to increase the Poisson's ratio to $\nu_{12} = -3.6$ for the same curvature ratio (Fig. 8-b). It is worth noticing that the absence of the curvature would lead to an even lower Poisson's ratio (-3).

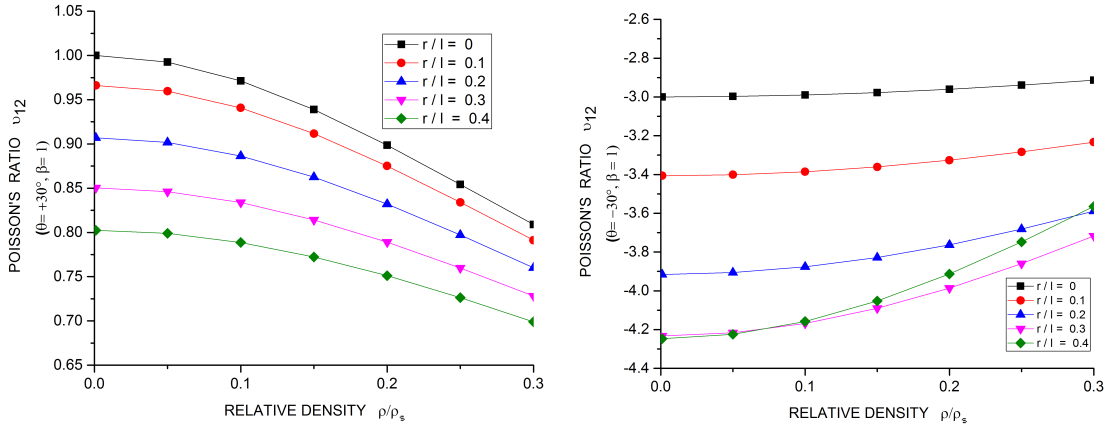

(a) (b)

Fig 8: Variation of the Poisson's ratio ν_{12} as a function of the relative density and curvature for different curvature ratios $\alpha = r/l$

For, $\beta = 1$. and an internal angle of the cell (a) $\theta = 30°$, (b) $\theta = -30$

IV.2. Analysis of the numerical results

The analytical model has been benchmarked against the data of the FE simulations. Fig. 9 compares the two sets of results related to the Poisson's ratio ν_{12} versus the relative density. The difference between the theoretical results and the numerical predictions is relatively small (1.5% maximum). For the convex case ($\theta = 30^o$), the FE simulations confirm the decrease of the Poisson's ratio with the increase of the relative density. More importantly, the FE data also confirm the decrease of the Poisson's ratio for positive values of the curvature ratio.

The longitudinal modulus of elasticity was calculated for different relative densities ranging from 0.01 for a thin wall to 0.3 for a thicker one. The cell aspect ratio β is fixed to 1. In all the cases examined, the FE model shows a significant correlation between the theoretical results with the parameter θ. An interesting observation can be made by looking at the curve

representing the anisotropy ratio E_1/E_2 and the Poisson's ratio ν_{12} versus the internal cell angle (Fig. 10). The presence of a radius of curvature (α=0.1) is sufficient to move the peak of the anisotropy ratio and the zero Poisson's ratio value to a negative internal cell angle (-6° in this case). The presence of a curved wall tends therefore to increase the stiffness ratio in the negative internal cell angle regime, and also to extend in that angle range the presence of positive or zero Poisson's ratio values. A classical configuration with no curved walls would have the location of the peak stiffness ratio and the zero Poisson's ratio exactly at θ=0° [34].

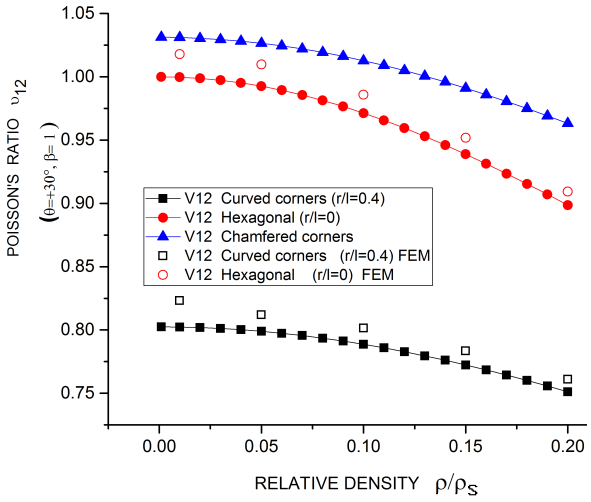

Fig. 9 Comparison between the analytical model and the FE simulation for the Poisson's ratio ν_{12}.(θ =30° ;β=a/l =1)

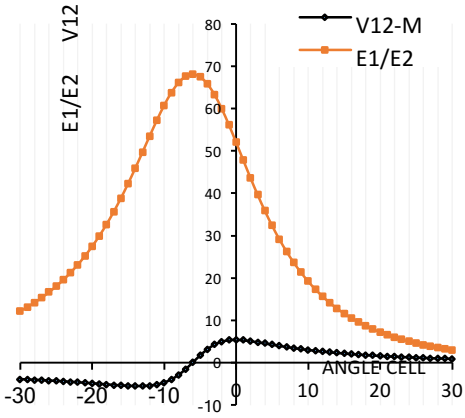

Fig.10 E_1/E_2 ratio and Poisson's ratio ν_{12}.versus the internal cell angle (α=r/l =0.1 ; β=a/l =1)

Table 1. Comparison of Poisson's ratio ν_{12} for the three cell configurations:
- curved corners *(r/l=0.4 , θ = 30°)* Hexagonal *(r/l=0 , θ = 30°)* chamfered corners ¶ for the same cell ¶

	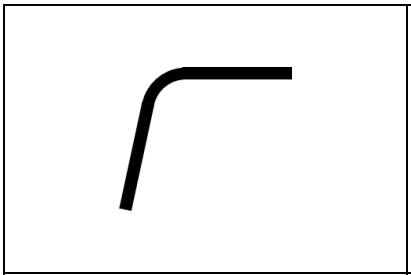			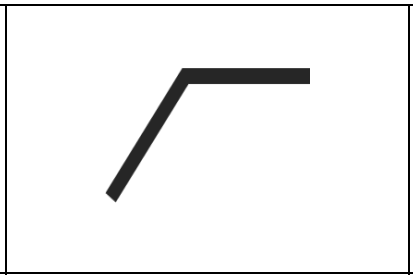			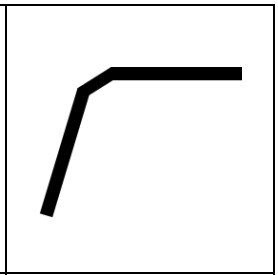	
	curved corners ν_{12} *(r/l=0.4 , θ = 30°)*			Hexagonal ν_{12} *(r/l=0, θ = 30°)*			chamfered corners ν_{12}	
ρ / ρ_s	$\gamma = t/l$	ν_{12}	ν_{12} (FEM)	$\gamma = t/l$	ν_{12}	ν_{12} (FEM)	$\gamma = t/l$	ν_{12}
0.01	0.0119	0.8023	0.8103	0.0087	0.9997	1.0178	0.0129	1.0310
0.05	0.0594	0.7989	0.8120	0.0433	0.9926	1.0098	0.0643	1.0265
0.10	0.1188	0.7887	0.8014	0.0866	0.9713	0.9859	0.1286	1.0127
0.15	0.1781	0.7724	0.7834	0.1299	0.9388	0.9519	0.1929	0.9911
0.20	0.2375	0.7512	0.7610	0.1732	0.8986	0.9094	0.2572	0.9631

Conclusions

The present work describes the geometry a centre symmetric honeycomb structure with internal curved cell walls. The honeycomb can also provide auxetic (in-plane Poisson's ratio) deformations with internal negative cell angles. The in-plane elastic constant of the honeycomb is modelled using an analytical approach based on Castigliano's theorem, and take into account all the three possible deformation mechanisms within the engineering beam theory – bending, stretching and shear deformation of the cross section. Compared to the classical centre symmetric honeycomb models, the curved wall honeycomb concept is defined by four geometries non-dimensional groups that include the curvature ratio. The theoretical uniaxial properties have been benchmarked against Finite Element simulations that reproduce the elastic constants of the honeycomb in an asymptotic homogenization approach.

Between the most remarkable features of this honeycomb design, one has to note the effect of the radius of curvature of the wall over the Poisson's ratio. While higher curvatures provide a decrease in the magnitude of the Poisson's ratio for convex cell configurations (i.e., positive internal cell angle), in re-entrant or auxetic configurations the effect is opposite: the magnitude of the negative Poisson's ratio is increased. The presence of curvatures also tends to shift towards negative cell angles the peak of in-plane uniaxial anisotropy and the switch between the negative and positive Poisson's ratio zones. For classical centre symmetric honeycomb configurations, the corresponding internal cell angle for this limit configurations is constant, and it is equal to zero. Curved walls in honeycombs design can therefore be efficiently used to tailor unusual equivalent mechanical properties in cellular solids.

References

[1]. M. Laroussi, Modeling the behavior of solid foams porosity: a micro mechanical approach, ph.D. l'ENPC Champs-sur-Marne, 2002.

[2]. L. J. Gibson, M. F. Ashby. *Cellular solids: structure and properties* (2nd.ed.UK, Cambridge university press, 1997).

[3]. M. J. Silva, W. C. Hayes, L. J. Gibson, The effects of non-periodic microstructure on the elastic properties of two-dimensional cellular solids, *Int. J. Mech. Sci.* 11 *(1995) 61–77.*

[4]. Wang ZG, Tian HQ, Lu ZJ, Zhou W. High-speed axial impact of aluminium honeycomb-experiments and simulations. Compos Part B 2014; 56:1–8

[5]. Masters, I.G., Evans, K.E., 1997. Models for the elastic deformation of honeycombs. Compos. Struct. 35, 403–422

[6]. Kelsey S, Gellatley RA, Clark BW. The shear modulus of foil honeycomb cores. Aircraft Eng 1958;30:294–302.

[7]. Bitzer, T. N. *Honeycomb Technology: Materials, Design, Manufacturing, Applications and Testing*. Springer Science & Business Media, 1997.

[8]. Nojima, T., and Saito, K., 2006. Development of Ultra-Light Core Structure. JSME International A, 49(1), pp.38

[9]. Saito, K., Agnese, F., and Scarpa, F. A Cellular Kirigami Morphing Wingbox Concept. 2011, Journal of Intelligent Material Systems and Structures, 22, pp.935-944.

[10]. Bezazi A, Scarpa F, Remillat C. A novel centre symmetric honeycomb composite structure. Compos Struct 2005;71:356–64.

[11]. K Boba, M Bianchi, G McCombe, R Gatt, A C Griffin, R M Richardson, F Scarpa, I Hamerton, J N Grima, 2016. Blocked shape memory effect in negative Poisson's ratio polymer metamaterials. ACS Applied Materials & Interfaces 8 (31), 20319-20328

[12]. [12]. [Str2016] T. Strek, H. Jopek, and K. W. Wojciechowski, "The influence of large deformations on mechanical properties of sinusoidal ligament structures," Smart Mater. Struct., vol. 25, no. 5, p. 54002, 2016.

[13]. [13] [Gri2013] J. N. Grima, R. Caruana-Gauci, K.W. Wojciechowski, K. E. Evans, Smart hexagonal truss systems exhibiting negative compressibility through

constrained angle stretching, Smart Mater. Struct. 22 (2013) 84015. doi:10.1088/0964-1726/22/8/084015.

[14]. [14] [Poz2013] A. A. Pozniak, J. Smardzewski, K. W. Wojciechowski, Computer simulations of auxetic foams in two dimensions, Smart Mater. Struct. 22 (2013) 84009. doi:10.1088/0964-1726/22/8/084009.

[15]. [15] [Str2015] T. Strek, H. Jopek, M. Nienartowicz, Dynamic response of sandwich panels with auxetic cores, Phys. Status Solidi. 252 (2015) 1540-1550. doi:10.1002/pssb.201552024.

[16]. [16] [Str2016] T. Strek, H. Jopek, E. Idczak, Computational design of two-phase auxetic structures, Phys. Status Solidi Basic Res. 253 (2016). doi:10.1002/pssb.201600120.

[17]. [Lakes 1987]

[18]. [18] [Lak1991] R. Lakes, Deformation mechanisms in negative Poisson ratio materials - structural aspects, J. Mater. Sci.,vol.26, no. 9, pp.2287-2292,1991.

[19]. [19] [Sig1994] O. Sigmund, Materials with prescribed constitutive parameters - an inverse homogenization problem, Int. J. Solids Struct., Vol. 31,no. 17 pp. 2313-2329, 1994

[20]. [20] [Miz2015] L. Mizzi, D. Attard, R. Gatt, Ruben Gatt, Artur A. Pozniak, Krzysztof W. Wojciechowski, Joseph N. Grima. Influence of translational disorder on the mechanical properties of hexachiral honeycomb systems, Compos. Part B-Eng., vol.80, pp. 84-91, 2015.

[21]. [21] [Jop2015] H. Jopek and T. Strek, Thermal and structural dependence of auxetic properties of composite materials, Phys. Status Solidi, vol. 252, no. 7, pp. 1551-1558, 2015.

[22]. [22] [Gri2016] J. N. Grima, L. Mizzi, K.M. Azzopardi, and Ruben Gatt et al., Auxetic perforated mechanical metamaterials with randomly oriented cuts, Adv. Mater.,vol.28, no.2, pp. 385-389, 2016

[23]. [23] [Poz2016] A.A. Pozniak, K.W. Wojciechowski, J.N. Grima, Luke Mizzi et al., Planar auxeticity from elliptic inclusions, Compos. Part B-Eng., vol.94, pp.379-388, 2016

[24]. [24] [Woj1987] K.W. Wojciechowski, Constant thermodynamic tension Monte-Carlo studies of elastic properties of a two-dimensional system of hard cyclic hexamers, Molecular Physics, vol.61, no.5, pp.1247-1258, 1987

[25]. [25] [Woj1989] K.W. Wojciechowski, Two-dimensional isotropic system with a negative Poisson ratio, Physics Letters A vol.137, no.1-2, pp.60-64, 1989.

[26]. [26] [Ish2000] Y. Ishibashi, M. Iwata, A Microscopic Model of a Negative Poisson's Ratio in Some Crystals, Journal of the Physical Society of Japan, vol. 69, no.8, pp.2702-2703, 2000.

[27]. [Bil2016] M. Bilski, K. W. Wojciechowski, Tailoring Poisson's Ratio by Introducing Auxetic Layers J. Phys. Status Solidi B, vol.253, no.7, pp.1318-1323, 2016

[28]. Zhang, J., Ashby, M.F., 1992. The out-of-plane properties of honeycombs. Int. J. Mech. Sci. 34,475–489.

[29]. Burton, W.S., Noor, A.K., 1997. Assessment of continuum models for sandwich panel honeycomb cores. Comput. Methods Appl. Mech. Eng. 145, 341–360.

[30]. Balawi, S., Abot, J.L., 2008. The effect of honeycomb relative density on its effective in-plane elastic moduli: An experimental study. Compos. Struct. 84, 293–299.

[31]. Sigmund O, and Torquato S. Design of smart composite materials using topology optimization, Smart materials and Structures 8 : 365-379 -1999

[32]. Lira C, Innocenti P, Scarpa F. Transverse elastic shear of auxetic multi reentrant honeycombs. Compos Struct 2009; 90:314–22.

[33]. ABAQUS, version CEA 6.10-1 reference manuals, Dassault Systemes, Providence, R.I: Abaqus Inc., 2010.
[34]. Scarpa F, Panayiotou P, Tomlinson G. Numerical and experimental uniaxial loading on in-plane auxetic honeycombs. The Journal of Strain Analysis for Engineering Design 35(5), 383-388.